Electron pickup from a free-electron gas by channeled heavy ions

S. A. Jackson and P. M. Platzman

Bell Laboratories, Murray Hill, New Jersey 07974

(Received 17 September 1979)

The transition rate is calculated for picking up a single-valence or free electron in a solid into the 1s and 2s hydrogenic states on a completely stripped ion of charge Z as the ion passes through a thin solid film in a given crystallographic direction between rows of atoms of charge Z'. The results exhibit a structure reminiscent of the Okorokov effect, which is explainable in terms of a lattice momentum transfer-dependent phase space. The possibility of directionally or energetically tuning maxima in the pickup fraction or detuning competing processes is suggested. Possible uses are indicated for a beam of (possibly polarized) high-Z metastables produced in this way in interesting experiments in atomic and weak-interaction physics.

I. INTRODUCTION

There has been much interest recently in two aspects of atomic collisions in solids: channeling and the emergent charge states of fast ions in solids. Channeling is the passing of a particle beam along a given crystallographic direction in a solid. Among other things, this process is being used extensively to study transitions between bound states on ions[1] (the Okorokov[2] effect) and to study the properties of surfaces of semiconductors.[3] Much of the work on charge states of fast ions in solids, including recent work by Cross,[4] has treated capture into and loss from bound states on the moving ion from target atom core levels (e.g., Auger processes). In this paper, we will calculate, within the framework of a simple model, the transition rate for the creation of a high-Z metastable arising from the pickup of a free (valence) electron into a bound state on a fully stripped ion of charge Z as it passes through a thin (< 2000 Å) solid film in a given crystallographic direction. From our simple calculation, we hope to get a good rough estimate of the size of the cross section and of its energy dependence.

The basic mechanism for the capture process is simple. As the stripped ion passes down its channel, it feels a coherent periodic potential produced by the rows of partially screened atoms in the solid. This potential has a basic set of frequencies, $\nu_n = n v/d$, where d is the periodicity of the atoms in a given direction. The quantity v is the velocity of the beam, and n is an arbitrary integer. Roughly speaking, when ν_n is equal to a specific energy difference, an electron may be captured into a bound state with the emission of a virtual photon.

Our interest in the problem is twofold. The process is interesting in its own right. It is a resonant nonradiative capture process. The way the cross section depends on energy and deviates from the simple

δ-function argument given above will depend on the details of the valence-electron velocity distribution on its wave function, and on the nature of the periodic potential. Such resonant capture processes may provide unique beams of metastables for doing a variety of atomic physicslike experiments after that beam emerges from the solid.

In the next section, we discuss the model we have used in our calculation. What should be borne in mind is that this is strictly a first attempt at calculating the structure to be expected in such a coherent capture process. When further data become available, the model may be refined.

II. MODEL

Before calculating the rate, we will first briefly list and discuss the assumptions in the calculation. (i) The electrons in the solid which are picked up are taken to be free electrons. This is a reasonable assumption for semiconductors like Si and for most metals, although for transition metals, the d electrons have considerable atomic character. We expect that the free-electron model will give a factor-of-two estimate of the cross section and of the smearing of the δ-function nature of the cross section due to initial-state velocity smearing (to be discussed in more detail). The initial wave function is assumed to be plane-wave-like. This assumption is quite good for the systems of interest, i.e., Z in the range of 8 to 17. In these cases, the hydrogenic binding ranges from 0.2 to 4 keV. For ion beam energies available (10–200 MeV), the energy of the valence electron (in the ion's rest frame) range from 5–100 keV. These energies are far enough above the binding energy that plane waves may be appropriate for describing them. (ii) The interaction between an electron and the moving ion is an unscreened Coulomb in-

teraction with charge Z. The effect of this interaction is embodied in the bound-electron wave function, which is taken to be hydrogenic. The potential experienced by an electron bound on a moving ion is made up of a Coulomb piece and exchange and correlation parts. There is negligible exchange between such an electron and core electrons in the solid because of deep binding and spatial separation due to the channeling effect. Exchange and correlation with the valence electrons are also small. Calculations by Neufeld and Ritchie[5] show that for a fast ion, the screening charge lags behind the ion by a distance v/ω_p, where ω_p is the characteristic frequency of long-wavelength modes in the solid; v is the ion's velocity. For v greater than a typical Fermi velocity, the solid cannot respond quickly enough to screen the ion ($v/\omega_p \gg a_H$, the effective Bohr radius). For this reason, exchange and correlation between an electron bound on the moving ions and valence electrons in the solid also is negligible. (iii) The perturbation which causes the transition is the periodic potential felt by the ion-electron system in passing along a particular channel in the solid. Since the Fermi-Thomas screening length for the conduction electrons is bigger than the channel dimension, we assume that the potential is unscreened Coulombic with charge Z'. The charge Z' is determined by the screening effects of the bound electrons in the solid. We use the results of Slater[6] to calculate Z' for various targets. Explicit exchange and correlation effects are small for the same reasons discussed in assumption (ii). (iv) The bound-electron orbit about the ion is assumed to be smaller than the channel dimension ($\approx$ lattice constant) in order to reduce reionization (checked *a posteriori*).

Of course, we have neglected all types of intrinsic many-body effects which lead to capture in other nonresonant channels, for example, those involving Auger-type shake-up processes.[7] Such effects in related processes such as x-ray photoemission produce several percent effects on the overall transition rate.

III. TRANSITION RATE

Let us consider the ion-electron situation visualized in Fig. 1. The ions are assumed to follow classical paths along which they feel the periodic potential of the atomic lattice. The potential at the point $\vec{R}$ is

$$V(\vec{R}) = \sum_l V(\vec{R} - \vec{R}_l)$$

$$= \sum_l \sum_{\vec{g}} V_{\vec{g}} e^{i\vec{g} \cdot (\vec{R} - \vec{R}_l)} \tag{1}$$

$$= \sum_{\vec{g}} \bar{V}_{\vec{g}} e^{i\vec{g} \cdot \vec{R}} ,$$

where $\vec{R}_l$ is the position of the lth atom in the crystal and $\vec{g}$ is the reciprocal-lattice vector of the solid. If V

CHANNELED ION-ELECTRON SYSTEM

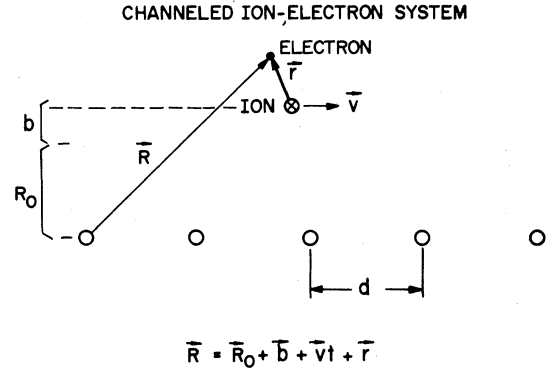$$\vec{R} = \vec{R}_0 + \vec{b} + \vec{v}t + \vec{r}$$

FIG. 1. Channeled ion-electron system.

is an unscreened Coulomb potential,

$$\bar{V}_{\vec{g}} = \frac{-4\pi Z' e^2}{v_c} \frac{1}{|\vec{g}|^2} = \frac{-4\pi Z' e^2}{v_c} \frac{1}{(\vec{g}_\perp^2 + g_\parallel^2)} , \tag{2}$$

where v_c is the volume of the unit cell of the crystal. The $\parallel$ direction is always defined by the direction of motion, in the solid, of the incoming ion which we always take to be along a crystal axis. For the situation of Fig. 1,

$$\vec{R} = \vec{r} + \vec{v}t + \vec{b} + \vec{R}_0 . \tag{3}$$

where $\vec{r}$ is the position of the electron relative to the moving ion, $\vec{v}t$ is the distance the ion has traveled in the $\parallel$ direction relative to some reference atom in the solid, $\vec{b}$ is the ion's transverse distance from the center of the channel, and $\vec{R}_0$ defines the center of the channel relative to the reference row of atoms. It does not matter which row is chosen as the reference since we sum over all atomic positions. We may then write the potential as

$$V(\vec{R}) = \sum_{\vec{g}_\perp} e^{i\vec{g}_\perp \cdot \vec{b}} \sum_{g_\parallel} V_{\vec{g}} e^{i\vec{g} \cdot (\vec{r} + \vec{v}t + \vec{R}_0)} . \tag{4}$$

The $e^{i\vec{g} \cdot \vec{R}_0}$ term contributes a phase factor which drops out when the transition probability is calculated.

The probability for a transition from the free state q to a bound atomic state n on the ion is given by

$$P_{nq}(t) = \frac{1}{\hbar^2} \left| \sum_{\vec{g}_\parallel} e^{-i(\omega/2)t} \frac{\sin\frac{1}{2}\omega t}{\frac{1}{2}\omega} U_{g_\parallel}^{nq} \right|^2 . \tag{5}$$

where

$$\omega = \frac{E_q - E_n}{\hbar} - \vec{g} \cdot \vec{v} = \omega_{nq} - \omega_0 \tag{6}$$

and

$$U_{g_\parallel}^{nq} = \sum_{\vec{g}_\perp} e^{i\vec{g}_\perp \cdot \vec{b}} V_{\vec{g}_\perp, g_\parallel} (e^{i\vec{g} \cdot \vec{r}})_{nq} . \tag{7}$$

The matrix element is taken between the states

$$\psi_q = \frac{1}{\sqrt{\Omega}} e^{i\vec{q}\cdot\vec{r}} \quad . \tag{8}$$

where Ω is the volume within which the plane wave is normalized, and

$$\psi_n = R_{nl}(r) Y_{lm}(\Theta, \phi) \quad . \tag{9}$$

In Eq. (10), the radial wave function is

$$R_{nl}(r) = 2 \left[\frac{Z}{a_0} \right]^{3/2} \frac{1}{n^2} \frac{(n-l-1)!^{1/2}}{(n+l)!} \left[\frac{2r}{na_0} \right]^l$$

$$\times e^{-r/na_0} L_{n-l-1}^{2l+1} \left[\frac{2r}{na_0} \right] \quad . \tag{10}$$

where $Y_{lm}(\Theta, \phi)$ is a spherical harmonic and $L_n^\nu(x)$ is a Laguerre polynominal. For the $1s$ and $2s$ hydrogenic states, we have

$$\psi_{1s} = \frac{1}{\sqrt{\pi}} \left[\frac{Z}{a_0} \right]^{3/2} \exp\left[\frac{-Zr}{a_0} \right] \tag{11}$$

and

$$\psi_{2s} = \frac{1}{4} \frac{1}{(2\pi)^{1/2}} \left[\frac{Z}{a_0} \right]^{3/2} \left[2 - \frac{Zr}{a_0} \right] \exp\left[\frac{-Zr}{2a_0} \right] \quad . \tag{12}$$

where

$$a_0 = \frac{\hbar^2}{\mu e^2} \quad . \tag{13}$$

which is equal to 0.53×10^{-8} cm (Bohr radius) and $\vec{q}$ is the wave vector of the electron $[\equiv (\mu/\hbar)(\vec{v}_e - \vec{v})]$ relative to the ion. The velocity $\vec{v}_e$ is the electron velocity in the laboratory and $\vec{v}$ is the ion velocity. The transition rate may be calculated in the usual manner as

$$W_{nq} = \frac{d}{dt} P_{nq}(t)$$

$$= \frac{2\pi}{\hbar} \sum_{g_\parallel} |U_{g_\parallel}^{nq}|^2 \delta(E_{\vec{q}} + \epsilon - \hbar\omega_0) \quad . \tag{14}$$

where $\epsilon = -|E_n|$ (E_n is the binding energy for the state n). We average over the possible initial states q to obtain

$$W = \sum_{\vec{q}} n_{\vec{q}} W_{nq} = \sum_{\substack{\vec{q} \\ (|\vec{v}_e| \leq v_F)}} W_{nq}$$

$$= \frac{\Omega}{(2\pi)^3} \int d\vec{q} \frac{2\pi}{\hbar} \sum_{g_\parallel} |U_{g_\parallel}^{nq}|^2 \delta(E_{\vec{q}} + \epsilon - \hbar\omega_0) \quad . \tag{15}$$

The factor $n_{\vec{q}}$ is the Fermi-Dirac occupation probability which we take to be one for $|\vec{v}_e| \leq v_F$, the Fermi velocity. We ignore the finite temperature smearing. Since

$$E_{\vec{q}} = \frac{1}{2}\mu(\vec{v}_e - \vec{v})^2 \approx \frac{1}{2}\mu v^2 - \mu v v_{e_\parallel} \quad .$$

Eq. (15) may be written as

$$W = \frac{\Omega}{(2\pi)^3} \frac{2\pi}{\hbar} \left[\frac{\mu}{\hbar} \right]^3 \sum_{g_\parallel} \int d\vec{v}_e |U_{g_\parallel}^{nq}|^2 \frac{1}{\mu v} \delta\left[\frac{1}{2}v - \frac{(\hbar\omega_0 - \epsilon)}{\mu v} - v_{e_\parallel} \right]$$

$$= \frac{\Omega}{(2\pi)^2} \frac{\mu^2}{\hbar^4} \frac{1}{v} \sum_{g_\parallel} \int d\vec{v}_{e_\perp} dv_{e_\parallel} |U_{g_\parallel}^{nq}|^2 \delta\left[\frac{1}{2}v - \frac{(\hbar\omega_0 - \epsilon)}{\mu v} - v_{e_\parallel} \right] \quad . \tag{16}$$

(Note: $\vec{v}$ is a vector quantity; v is an absolute value.) At this point, it is worthwhile to note the following. Normally, the energy-conserving δ function, $\delta(E_{\vec{q}} + \epsilon - \hbar\omega_0)$, (with E_q being the free-electron energy) would mean that $g_\parallel$ could vary over an infinite range (since $\hbar\omega_0 = \hbar g_\parallel v$). However, since we are dealing with valence electrons, in the laboratory frame, we have $\frac{1}{2}\mu v_e^2 \leq E_F$ (the Fermi energy), or $|\vec{v}_e| \leq v_F$. Therefore

$$(\vec{v}_{e_\perp})^2 + (v_{e_\parallel})^2 \leq v_F^2 \tag{17}$$

and

$$\int d\vec{v}_{e_\perp} = [\vec{v}_F^2 - (v_{e_\parallel})^2] \quad . \tag{18}$$

The resulting integration yields

$$W = \sum_{g_\parallel} \frac{(v_F^2 - v_m^2)}{vd} \frac{Z^5 Z'^2 \Re^2}{4\pi^6 \epsilon_d^2} \left[\frac{d}{a_0} \right]^3 |F_{g_\parallel}|^2 \quad . \tag{19}$$

where

$$|U_{g_\parallel}^{nq}|^2 = 4Z^5 Z'^2 \Re^2 \frac{d^3}{\Omega} \left[\frac{d}{a_0} \right]^3 |F_{g_\parallel}|^2 \quad . \tag{19a}$$

with $\epsilon_d = (\hbar^2/2\mu d^2)$, $\Re = $ rydberg ($= 13.6$ eV), and

$$v_m = v_{e_\parallel} = \frac{\frac{1}{2}\mu v^2 + \epsilon - mh v/d}{\mu v} \quad . \tag{20}$$

if $g_\parallel$ is written $(2\pi/d)m$, where d is the periodicity in the direction of ion motion in the crystal. The sum on m is restricted by the constraint that $|\vec{v}_e| \leq v_F$ which gives

$$\frac{\frac{1}{2}\mu v^2[1-(2v_F/v)]+\epsilon}{hv/d} \leq m \leq \frac{\frac{1}{2}\mu v^2[1+(2v_F/v)]+\epsilon}{hv/d} \quad ; \tag{21}$$

m takes on integer values within this range. The values of the m's increase as v (or ion energy) increases.

For a transition from the free state to, e.g., the $2s$ state on the ion, if we average over possible impact parameters (since the precise impact parameter of a given ion is unknown), we obtain

$$|F_{g_\parallel}|^2 = \sum_{k,l} \frac{1}{(m^2+k^2+l^2)^2} \left[\frac{1}{(\rho^2+k^2+l^2)^2} - \frac{\frac{1}{2}\alpha^2(d/2\pi)^2}{(\rho^2+k^2+l^2)^3} \right]^2 . \tag{22}$$

for the simple cubic lattice with ion beam traveling in the [100] direction. In deriving this expression, we assume a flat distribution of impact parameters across the channel (i.e., equal weight to each impact parameter). This results in a δ function when the averaging is done, which eliminates the cross terms in the sum over $\bar{g}_\perp$. However, it is known that the channeled ions tend to be clustered near the center of the channel with a falloff of intensity near the channel edges. Based on discussions with Appleton,[9] we also used a Gaussian distribution of impact parameters with a width adjusted to give the proper falloff at the channel edges. When the averaging is done with this distribution, we end up with a Gaussian interference term in the sum over $\bar{g}_\perp \{\sim \exp[-(\bar{g}_\perp-\bar{g}'_\perp)^2\frac{1}{4}\lambda^2]\}$ with a width, $1/\lambda$, inversely proportional to the channeled beamwidth. This function is peaked at $\bar{g}_\perp = \bar{g}'_\perp$, and falls off rapidly for momentum transfer differences greater than the inverse width of the ion beam. We expect the results to be very similar to those for a flat momentum distribution since our typical $\bar{g}_\perp$ is larger than the inverse of the channeled beamwidth. For an fcc lattice with ion beam traveling in the [110] direction, we obtain

$$|F_{g_\parallel}|^2 = \sum_{k,l} \frac{1}{[m^2+\frac{1}{2}(m-k-l)^2+(k-l)^2]^2} \left[\frac{1}{[\rho^2+\frac{1}{2}(m-k-l)^2+(k-l)^2]^2} - \frac{2(\alpha d/4\pi)^2}{[\rho^2+\frac{1}{2}(m-k-l)^2+(k-l)^2]^3} \right]^2 . \tag{23}$$

These expressions result because

$$\bar{g}_\perp^2 = \left[\frac{2\pi}{d}\right]^2 (k^2+l^2) . \tag{24a}$$

$$g_\parallel^2 = \left[\frac{2\pi}{d}\right]^2 m^2 . \tag{24b}$$

for the simple-cubic case, analogously for the fcc case. In Eqs. (22) and (23)

$$\rho^2 \equiv \left[\frac{\alpha d}{4\pi}\right]^2 + \left[\frac{\epsilon-\frac{1}{2}\mu v^2}{hv/d}\right]^2 . \tag{25}$$

where $\alpha = Z/a_0$. The expression for $|F_{g_\parallel}|^2$ for other crystal structures and beam directions can be worked out easily. Now, $g_\parallel$ can always be written, $g_\parallel = (2\pi/d)m$, and

$$v_m = \frac{\frac{1}{2}\mu v^2 + \epsilon - \hbar g_\parallel v}{\mu v} . \tag{25a}$$

Since $|v_m| \leq v_F$, this leads to a quasiresonance condition in that only one or a few values of $g_\parallel$ will satisfy both the energy-conserving δ-function condition, $\delta(E_{\bar{q}}+\epsilon-h\omega_0)$, and the constraint $|\bar{v}_e| \leq v_F$.

We have written a simple program to calculate the transition rate for various cases by summing over the restricted set of m's (for a sequence of incoming ion energies—this tunes v) and over k and l. We calculate the transition rate for a gold target (of the fcc structure) with incoming ion beams in the [110] and [111] directions, and a graphite target (of the hcp structure) with incoming ion beams in the [001] direction and along a crystal axis in the basal plane, the $[\hat{a}]$ direction, where $\hat{a} = \frac{3}{2}\hat{x} + \frac{1}{2}\hat{y}$. We consider several cases: two beams of completely stripped (O^{8+}, Cl^{17+}) ions impinging at various energies on

TABLE I. Input parameters for pickup rate calculation.

Ion	Z	A	
	8 (O^{8+})	16.0	
	17 (Cl^{17+})	35.4	
Target	$v_F(10^8$ cm/sec$)$	a (Å)	Z'
	1.39 (Au)	4.08	3.7
	2.75 (C:graphite)	2.456	3.25
		6.696(c)	

gold and graphite targets and picking up electrons into the $1s$ and $2s$ states. In Table I, we present the parameters necessary for the calculation of a transition rate for a number of targets. The calculation requires as input the following: (i) the maximum number of terms to be considered in the k and l sums, which we pick to get good convergence (for the cases considered, we take $k_{max} = l_{max} = 20$); (ii) the Fermi velocity of electrons in the target, v_F; (iii) the charge of the ion Z; (iv) the effective charge of the target atoms as seen by the valence electrons, Z'; (v) the lattice constants, a, c; (vi) the atomic weight of the ion, A; (vii) the energy of the ion beam, E_I.

IV. RESULTS

The results are summarized in Figs. 2 to 6. We plot the fraction $(=WL/v$, L is target thickness), versus energy, of the ions in the incoming beam which have picked up an electron into the bound state considered traveling through a target ~ 1000 Å thick. The fraction will scale linearly as the sample thickness until reionization by some process begins to become appreciable. Given the computed yields (see
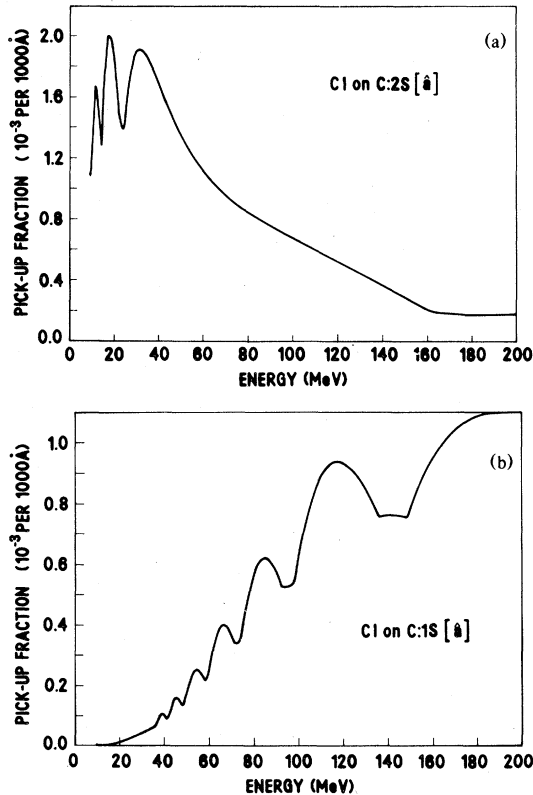

FIG. 2. (a) $2s$ pickup fraction vs energy, for chlorine impinging on graphite in $[\hat{a}]$ direction; (b) $1s$ pickup fraction vs energy, for chlorine impinging on graphite in $[\hat{a}]$ direction.
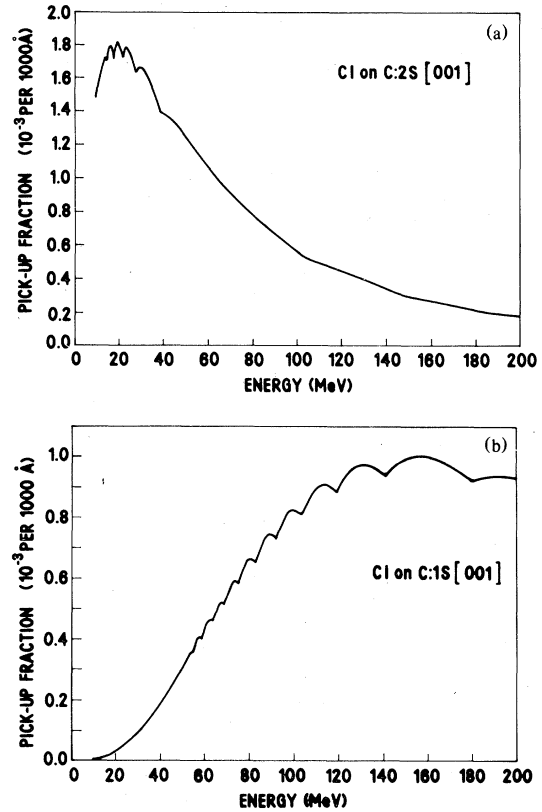

FIG. 3. (a) $2s$ pickup fraction vs energy, for chlorine impinging on graphite in [001] direction; (b) $1s$ pickup fraction vs energy, for chlorine impinging on graphite in [001] direction.

Figs. 2 to 6), reionization by the same process is clearly unimportant until one gets to sample thicknesses of several hundred thousand angstroms thick. We must, however, consider the possibility of reionization by collisions between the free-electron gas and the metastables. Rough estimates using calculated cross sections taken from Mott and Massey[8] indicate that the mean free path for reionization is between five and ten thousand angstroms, depending on target and beam energy.

The following features of the resultant curves for the pickup fraction may be noted. For each target and ion beam interaction, there exists a broad maximum at $\epsilon \sim \frac{1}{2}\mu v^2$ ($\epsilon = -E_n$, binding energy on the ion). This is just the Bohr condition. The maximum in the pickup fraction is actually shifted down in energy because of division of the transition rate by v. The width of this maximum is proportional to $(\alpha d/n)^2$. The larger $(\alpha d)^2$ is, i.e., the broader the Bohr peak, the larger d is relative to the effective Bohr radius which implies a better fit into the channel. There exists a series of minima (secondary maxima) which are regularly spaced (see curves for tran-
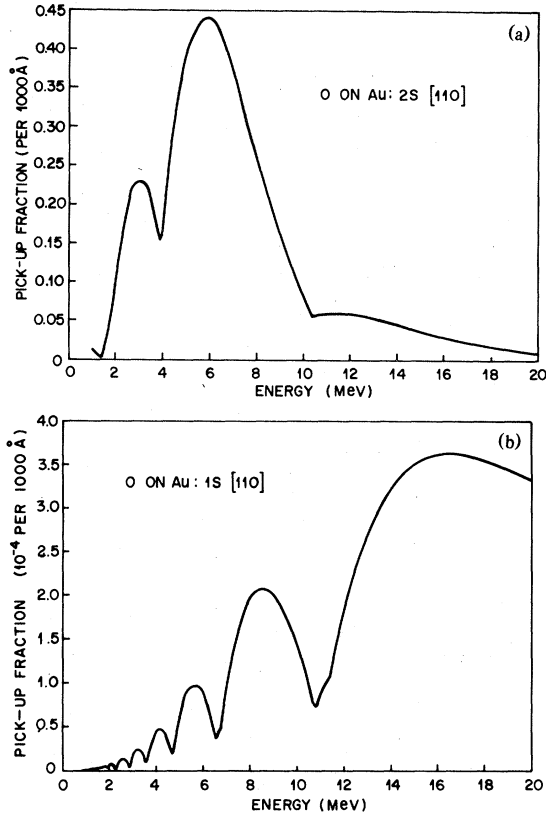
FIG. 4. (a) $2s$ pickup fraction vs energy, for oxygen impinging on gold in [110] direction; (b) $1s$ pickup fraction vs energy, for oxygen impinging on gold in [110] direction.

FIG. 5. (a) $2s$ pickup fraction vs energy, for oxygen impinging on gold in [111] direction; (b) $1s$ pickup fraction vs energy, for oxygen impinging on gold in [111] direction.

sitions to the $1s$ state). The spacing of the minima increases with increasing ion energy. Each minimum is really a double minimum. There is more structure in the curves for transition to the $1s$ state on the ion than to the $2s$ state. We note the existence of a number of minima in the $2s$ pickup fraction in the vicinity of, but below the Bohr resonance, particularly for chlorine on carbon. This is explained in the Appendix.

Finally, there are shallower minima for beam direction along [111] than along [110] and shallower minima for beam direction along [001] than along $[\hat{a}]$ for a given ion beam and target, and shallower minima for a carbon target than a gold target. If, for example, we consider the transition to the $1s$ state for oxygen impinging on a gold target [Figs. 4(b) and 5(b)], each minimum decreases the pickup fraction from the closest maximum value by a factor of $\sim 60\%$ for the [110] ion beam direction versus $\sim 4\%$ for the [111] direction. Similarly, for chlorine impinging on a graphite target (Figs. 2 and 3), the corresponding reductions are $\sim 40\%$ for $[\hat{a}]$ vs $\sim 7\%$ for [001]. For the case of chlorine impinging on graphite [Fig. 2(b)] in the $[\hat{a}]$ direction, the reduction is $\sim 40\%$ while for chlorine impinging on gold [Fig. 6(b)] in the [110]
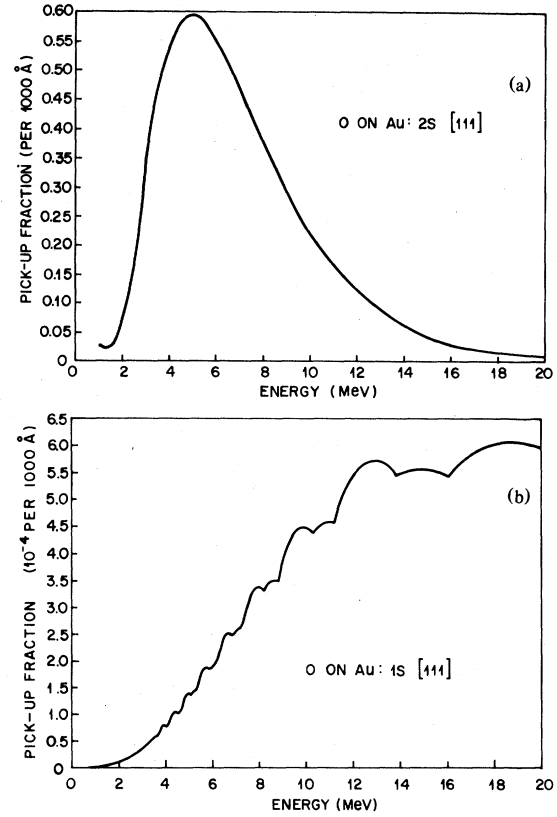
direction, the reduction is $\sim 77\%$.

Most features of our curves for the pickup fraction pertaining to the minima (secondary maxima) are explainable in terms of the available phase space for the process, which is given by the factor $v_F^2 - v_m^2$ in Eq. (19) for the transition rate. The minima occur where $v_m^2 = v_F^2$ or

$$\frac{1}{2}\mu(v \pm v_F)^2 + \epsilon - \frac{h v}{d} m = 0 \ , \tag{26}$$

from the energy-conserving δ function. This leads to the result that, at the minima,

$$v = \frac{1}{\mu}\left\{\left[\frac{h}{d} m \pm \mu v_F\right] + \left[\left[\frac{h}{d} m \pm \mu v_F\right]^2 - 2\mu\epsilon\right]^{1/2}\right\} \ , \tag{27}$$

this gives the closely spaced double minima observed in Figs. 4(b) and 5(b). The smaller $h/\mu v_F d$ is, the more closely spaced are these minima. If we recall that

$$\frac{\frac{1}{2}\mu v^2[1 - (2v_F/v)] + \epsilon}{h v/d} \leq m$$

$$\leq \frac{\frac{1}{2}\mu v^2[1 + (2v_F/v)] + \epsilon}{h v/d} \ , \tag{28}$$
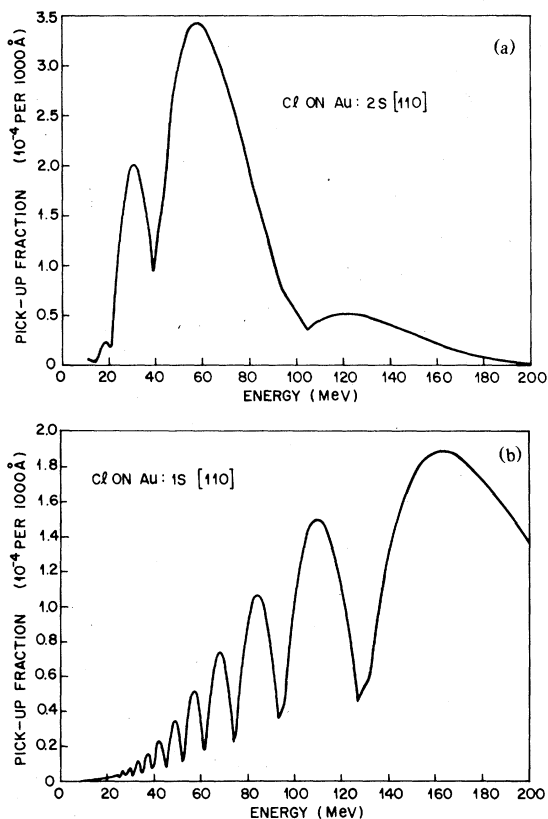
FIG. 6. (a) $2s$ pickup fraction vs energy, for chlorine impinging on gold in [110] direction; (b) $1s$ pickup fraction vs energy, for chlorine impinging on gold in [110] direction.

TABLE II. The range of reciprocal-lattice vectors for [111] and [110] beam directions ($\Delta m = 2\mu v_F d / h$).

Direction	$v_F (10^8$ cm/sec)	d (Å)	Δm
[111]	1.39 (Au)	7.07	2.70
[110]	1.39 (Au)	2.88	1.10
[001]	2.75 (C)	6.696	5.06
[$\hat{a}$]	2.75 (C)	2.456	1.85

m an integer, we can explain the observed features.

The spacing of the minima increases with increasing ion energy because as we sweep the ion energy, i.e., as we increase v, we reach a range of m, defined by Eq. (28), such that for an m in this range, for the given energy, the phase space vanishes. The velocity at this point is given by Eq. (27). Since

$$\left[\frac{h}{d}(m+1) + \mu v_F\right]^2 - \left[\frac{h}{d}m + \mu v_F\right]^2$$

is proportional to m for large m, the spacing between points where the phase space vanishes becomes larger as the ion energy increases, so the minima are more spread out.

There is more structure (more minima) in the pickup fraction curves for the transition to a $1s$ state than to a $2s$ state because the binding energy, ϵ, is larger for the $1s$ state than the $2s$ state. Looking at Eq. (27) for larger ϵ, the square-root term is smaller. The distance between successive values of v where $v_F^2 - v_m^2 = 0$ is smaller, hence more minima.

The minima for a [111] ([001]) ion beam direction are shallower than those for a [110] ([$\hat{a}$]) ion beam

direction for a given ion and target, and those for a carbon target are shallower than those for a gold target because for the shallower case, the range of m (i.e., how many terms in m must be summed) is larger than in the other case. With more terms contributing to the sum, there could be a minimum in one term, but summing over the other terms could mitigate the effect of this minimum, leading to a shallower dip. Note that the difference between the maximum and minimum values of m is given, independently of the ion energy, by

$$\Delta m = \frac{2\mu v_F d}{h} . \tag{29}$$

Values of Δm for gold (carbon) targets with ion beams along [111] ([001]) and [110] ([$\hat{a}$]) are given in Table II. If d is larger [as it is for [111] ([001]) beam direction relative to [110] ([$\hat{a}$]) beam direction], there are more terms in the m sum, leading to shallower minima [e.g., see Figs. 4(b) and 5(b): oxygen on gold [111] vs [110]]. Similarly, if v_F is larger for one target material than another (carbon versus gold), a wider range of m's will contribute and the material with a larger Fermi velocity will have shallower minima for a given projectile [cf. Figs. 2(b) and 4(b)].

V. DISCUSSION

Recently, Appleton et al.[9] have done work on radiative electron capture by oxygen ions in single-crystal channels in silver and silicon. They consider the capture of a free or weakly bound electron into the ground state on the oxygen ion (10–40 MeV) via photon emission. For this reason, they focus on their photon spectrum between 1 and 2 keV for 27.78 MeV O^{7+} on Ag[011] and 40 MeV O^{8+} on Si[011]. They find peaks in this region corresponding to energies $\sim Z^2 \Re + (\mu/M_I)E_I$ where Z, M_I, and E_I are the ion's charge, mass, and energy, and $\Re$ is the Rydberg energy. They argue that these peaks correspond to the transition of interest (free → $1s$). They calculate cross sections to be of the order of 10^{-22}–10^{-21} cm^2. Our mechanism would also cause this capture, but

would not be directly observable to photon emission, although the cross sections are comparable. The 2s capture process would, however, be observable by an allowed one-photon decay to the 1s ground state since the 2s state is mixed with the 2p state inside the crystal. We believe the authors in Ref. 9 have seen evidence for such an effect in these data. They also observed a peak in the channeled ion-photon spectra (uncorrected for absorption effects) for 27.78 MeV O^{7+} on Ag[011] and 40 MeV O^{8+} on Si[011] at a photon energy ~0.65−0.70 keV, which is not present in the nonchanneled experiments. The energy of this peak is essentially the energy difference between the 2s and 1s bound states on O^{8+}. The size of the cross section estimated from the intensity of this peak is about equal to that of the higher-energy one. Although it is not shown, we believe this lower-energy enhancement will remain even with absorption corrections. If this is the correct interpretation, then a study of the energy and/or channel dependence of its intensity should reveal all of the structure presented here. The effect could also be observed by studying the energy dependence of the emergent charge fractions.

Assuming that the cross sections and rough energy dependence reported here are correct, then such beams of metastables could be used in several different atomic-physics-type experiments.

Recent Lamb shift measurements on high-Z atoms[10] are probing the validity of electrodynamic calculations in strong external fields. These experiments are at present marginal. Any improvement by as much as one order of magnitude in signal-to-background would make these experiments useful. Currently, beams are prepared in nonchanneling geometries. The major signal-to-background problem arises because of the population of many unwanted He- and Li-like charge states. The process proposed here, or perhaps some variant of it, could be used to eliminate background and to improve count rates by about a factor of 10.

Another interesting feature of our process is the possibility of producing by pickup from a polarized electron gas, like Ni, polarized metastables. Since the pickup process is Coulombic, i.e., nonrelativistic, the electrons in the valence band will retain their polarization direction. Such polarized metastables could practically be used to study the parity-violation effects in electromagnetic interactions.[11] For example, a measurement of the anisotropy of the one-photon decay of the polarized 2s state would be a direct measure of such effects, and could possibly be feasible with the intensities reported here.

ACKNOWLEDGMENTS

APPENDIX

The minima in the 2s fraction near the Bohr resonance may be explained as follows. Looking at Eqs. (22) and (23) for the 2s transition in a cubic solid, we see that there exists the possibility of a minimum whenever a term in the k and l sums is such that

$$\left| 1 - \frac{2(\alpha d/4\pi)^2}{\rho^2 + f(m,k,l)} \right| = 0 \quad . \tag{A1}$$

where $f(m,k,l)$ gives the appropriate dependence on the momentum transfer from the lattice. This occurs whenever

$$f(m,k,l) = \left[\left(\frac{\alpha d}{4\pi} \right)^2 - \left(\frac{\epsilon - \frac{1}{2}\mu v^2}{h v/d} \right)^2 \right] \quad . \tag{A2}$$

Since $f(m,k,l)$ is positive, this equation can be satisfied at various points provided that $\frac{1}{2}\mu v^2 \lesssim \epsilon$, so that the second term on the right-hand side of Eq. (A2) is small or at least does not exceed the first.

---

[1]C. D. Moak *et al.*, Phys. Rev. A <u>19</u>, 977 (1979) and references cited therein.

[2]V. V. Okorokov *et al.*, Phys. Lett. A <u>43</u>, 485 (1973); S. Shindo and Y. H. Ohtsuki, Phys. Rev. B <u>14</u>, 3929 (1976).

[3]L. C. Feldman, Bell Telephone Laboratories Seminar entitled The Surface Peak Observed in Backscattering-Channeling and its Application to W(001) Reconstruction and the Si/SiO2 Interface (unpublished); L. C. Feldman, P. S. Silverman, J. S. Williams, T. E. Jackman, and J. Stensgaard, Phys. Rev. Lett. <u>41</u>, 1396 (1978).

[4]M. C. Cross, Phys. Rev. B <u>15</u>, 602 (1977).

[5]J. Neufeld and R. H. Ritchie, Phys. Rev. <u>98</u>, 1632 (1955).

[6]J. C. Slater, Phys. Rev. <u>36</u>, 57 (1930).

[7]P. H. Citrin, G. K. Wertheim, and Y. Baer, Phys. Rev. B <u>16</u>, 4256 (1977); P. H. Citrin, G. K. Wertheim, and M. Schlüter, *ibid.* <u>20</u>, 3067 (1979).

[8]N. F. Mott and A. S. W. Massey, *The Theory of Atomic Collisions* (Oxford University Press, New York, 1949).

[9]B. R. Appleton *et al.*, Phys. Rev. B <u>19</u>, 4347 (1979), and (private communication).

[10]D. E. Murnick, C. K. N. Patel, M. Leventhal, O. R. Wood II, and H. W. Kugel, J. Phys. (Paris) Colloq. <u>1</u>, C-34 (1979); H. W. Kugel and D. E. Murnick, Rep. Prog. Phys. <u>40</u>, 297 (1977) and references cited therein.

[11]Based on discussion of parity-violating effects in atoms by G. Feinberg and M. Y. Chen, Phys. Rev. D <u>1</u>, 190 (1974); G. Feinberg, Nature <u>271</u>, 509 (1978).